Editors' Suggestion | Featured in Physics

Nonvolatile Switching of Large Nonreciprocal Optical Absorption at Shortwave Infrared Wavelengths

Kenta Kimura[1,*] and Tsuyoshi Kimura[2]
[1]Department of Materials Science, Osaka Metropolitan University, Osaka 599-8531, Japan
[2]Department of Applied Physics, The University of Tokyo, Tokyo 113-8656, Japan

(Received 14 May 2023; revised 7 October 2023; accepted 6 December 2023; published 17 January 2024)

We report large nonreciprocal optical absorption at shortwave infrared (SWIR) wavelengths in the magnetoelectric (ME) antiferromagnet (AFM) $LiNiPO_4$. The difference in absorption coefficients for light propagating in opposite directions, divided by the sum, reaches up to ~40% at 1450 nm. Moreover, the nonreciprocity is switched by a magnetic field in a nonvolatile manner. Using symmetry considerations, we reveal that the large nonreciprocal absorption is attributed to Ni^{2+} *d-d* transitions through the spin-orbit coupling. Furthermore, we propose that an even larger nonreciprocity can be achieved for a Ni-based ME AFM where electric dipoles of every NiO_6 unit and Ni^{2+} spins are orthogonal and, respectively, form a collinear arrangement. This study provides a pathway toward nonvolatile switchable one-way transparency of SWIR light.

DOI: 10.1103/PhysRevLett.132.036901

Optical absorption or transparency of ordinary materials is symmetric with respect to a reversal of light propagation vector between $+\mathbf{k}$ and $-\mathbf{k}$. By contrast, when space-inversion and time-reversal symmetries of materials are both broken, the optical absorption can be different for $+\mathbf{k}$ and $-\mathbf{k}$ (inset in Fig. 1) [1–18]. This unconventional nonreciprocal optical absorption is called the optical diode (OD) effect by analogy with the semiconducting diode [10,12] and has received interest in view of potential applications to novel nonreciprocal optical devices controlling the light propagation. Thus far, OD effects have been observed in wide wavelength regions ranging from visible light to microwave. However, for the shortwave infrared (SWIR) region (typically 900 to 1700 nm) [19], which is part of the broadly defined near-infrared region (700 to 2500 nm) [20], there have been only a few reports [6,8,18] on the OD effects (see Fig. 1). Moreover, the reported effects are small [6,8] or require high magnetic fields to amplify the magnitude [18]. The SWIR region has been used for various applications including life science and telecommunications. Thus, the discovery of a nonvolatile (spontaneous) OD effect free from external fields in the SWIR region will be of great interest.

From the symmetry point of view, the OD effects can arise in a system with both chirality and magnetization ($\mathbf{M}$) for $\mathbf{k}\|\mathbf{M}$ and a system with a noncollinear configuration of electric polarization ($\mathbf{P}$) and $\mathbf{M}$ for $\mathbf{k}\|(\mathbf{P}\times\mathbf{M})$ [2,3]. Unfortunately, both chiral ferromagnets and polar ferromagnets are rather scarce, so that spontaneous OD effects related to $\mathbf{M}$ are rarely observed. By contrast, spontaneous OD effects can also arise in magnetoelectric (ME) antiferromagnets (AFMs), where antiferromagnetic spin ordering breaks both space-inversion and time-reversal symmetries because magnetic ions are placed on locally

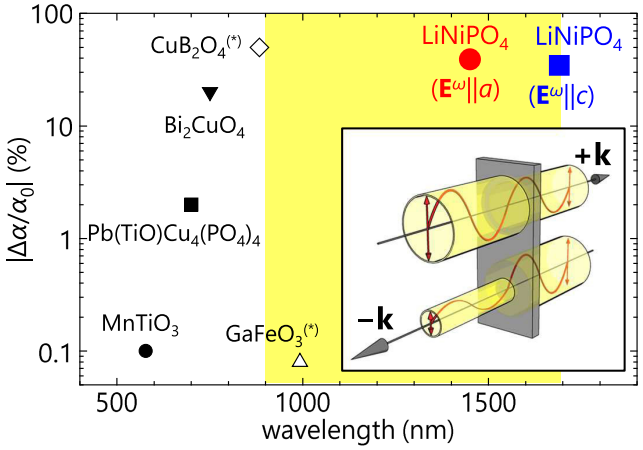

FIG. 1. Semilogarithmic plot of the magnitudes ($|\Delta\alpha/\alpha_0|$) of the spontaneous optical diode (OD) effect or closely related effects (nonreciprocal directional or linear dichroism and magnetochiral dichroism) in the visible to near-infrared regions for various materials including $LiNiPO_4$ investigated here (see the text), $MnTiO_3$ (wavelength of 577 nm, $|\Delta\alpha/\alpha_0| = 0.1\%$) [15], $Pb(TiO)Cu_4(PO_4)_4$ (700 nm, 2%) [16], Bi_2CuO_4 (750 nm, 20%) [17], $GaFeO_3$ (992 nm, 0.08%) [6], CuB_2O_4 (883 nm, 50%) [7]. For each material, the largest magnitude of $|\Delta\alpha/\alpha_0|$ is plotted. The asterisks on $GaFeO_3$ and CuB_2O_4 mean that the magnitudes for these materials were obtained in a weak but finite applied magnetic field: For $GaFeO_3$ a spontaneous $|\Delta\alpha/\alpha_0|$ should be finite but was not reported in the literature [6], while for CuB_2O_4 $|\Delta\alpha/\alpha_0|$ at a zero field is largely reduced compared to that in a weak field possibly due to randomization of magnetic domains [7]. The yellow background highlights the SWIR region. The inset illustrates the OD effect featured by a difference in the optical absorption between two counterpropagating light beams. The orientation and length of the red double headed arrows denote the polarization direction and the intensity of light, respectively.

inversion broken sites [13,15,17,21–24]. ME AFMs are much more common than chiral or polar ferromagnets. Therefore, ME AFMs are promising candidates to explore a large spontaneous OD effect in the SWIR range. Furthermore, achieving a large spontaneous SWIR OD effect in AFMs would greatly contribute to a rapidly growing research field of antiferromagnetic spintronics [25,26].

In this Letter, we propose and experimentally demonstrate that ME AFMs with NiO_6 octahedra can exhibit a giant spontaneous OD effect in the SWIR region, which corresponds to photon energies of Ni^{2+} d-d transitions. The NiO_6 octahedra are rather familiar and widely found in organic and inorganic compounds. Thus, the present study suggests Ni-based ME AFMs to be components of novel nonreciprocal devices of the SWIR region.

Microscopically, the OD effect originates from an interference between electric dipole (E1) and magnetic dipole (M1) transitions. Therefore, it will be largely enhanced when the E1 and M1 amplitudes are comparable to each other [2,6,7,11,14–17]. For visible to near-infrared regions including the SWIR region, such a situation may be achieved at a resonance of an electronic d-d transition of a magnetic ion with a particular ligand environment. Indeed, d-d transitions of Cu ions surrounded by square planar oxygens (CuO_4 unit) give rise to a large spontaneous OD effect of visible light in the ME AFM Bi_2CuO_4 [17]. In the present study, we pay attention to NiO_6 octahedral units in Ni-based ME AFMs because their lowest energy d-d transition ($^3A_{2g} \rightarrow {}^3T_{2g}$ in an O_h symmetry notation) is in the SWIR region [27]. In most cases, an oscillator strength of an M1 transition is much weaker than that of an E1 transition. For the $^3A_{2g} \rightarrow {}^3T_{2g}$ transition, by contrast, a significant M1 contribution was suggested on several Ni-based oxides [18,28–31], which is related to the fact that it is E1 forbidden but M1 allowed for a pure O_h symmetry. On this basis we anticipate that the M1 transition can be comparable in magnitude to the E1 transition, potentially leading to a giant OD effect. To demonstrate this possibility, we have taken $LiNiPO_4$ (space group $Pnma$) as a representative ME AFM consisting of NiO_6 units [see Fig. 2(a)]. $LiNiPO_4$ exhibits a second-order phase transition to an intermediate incommensurate (IC) antiferromagnetic phase at $T_{N2} = 21.7$ K, followed by a sharp first-order phase transition to a low-temperature commensurate (LTC) antiferromagnetic phase at $T_{N1} = 20.8$ K [32,33]. As shown in Fig. 2(a), the Ni^{2+} spins in the LTC phase are predominantly oriented along the crystallographic c axis with a small canting towards the a axis by $\theta_S = \pm(7.8° \pm 2.6°)$ [34,35]. This fully compensated antiferromagnetic structure belongs to magnetic point group $mm'm$ (m' is perpendicular to the b axis), breaks both space-inversion and time-reversal symmetries [36], and allows for a spontaneous OD effect for light propagating along the b axis ($\mathbf{k} \| b$), although its observation has not been reported to date.

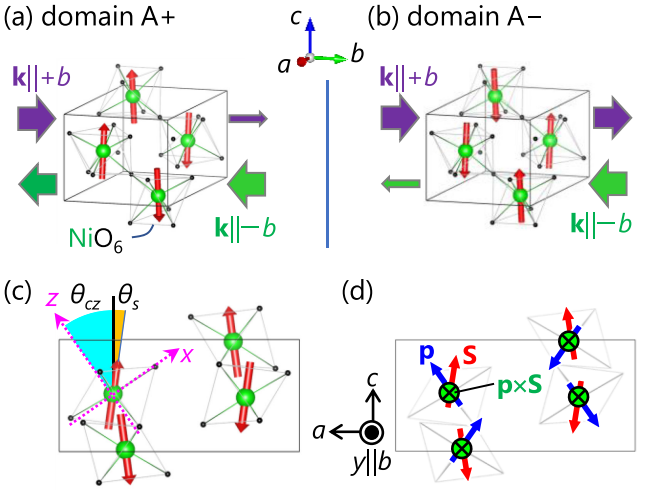

FIG. 2. (a),(b) Three-dimensional views of crystal and magnetic structures of $LiNiPO_4$ for a pair of antiferromagnetic domains A+ (a) and A− (b). Only Ni (green balls) and O atoms (black balls) are depicted for clarity. Red arrows denote Ni^{2+} spins. The unit cell (gray box) contains four distorted NiO_6 octahedral units, which are crystallographically equivalent to each other. The two domains can exhibit the OD effect of opposite signs, as represented by purple and green arrows whose thickness denote the intensity of light. (c) A b-axis view of the crystal and magnetic structures, indicating that the symmetry of NiO_6 is approximated as $2_z m_x m_y$, where x, y, and z denote local coordinate axes on each NiO_6 unit. $\theta_{cz} \approx 35°$ is an angle between c and z. Each Ni spin is predominantly oriented along the c axis but cants towards the a axis by an angle $\theta_S = \pm(7.8° \pm 2.6°)$. (d) Geometrical relationship among a local electric dipole $\mathbf{p}$ along the z axis (blue arrows), the Ni^{2+} spin $\mathbf{S}$ (red arrows), and a quantity $\mathbf{p} \times \mathbf{S}$ (green crosses). The quantity $\mathbf{p} \times \mathbf{S}$ on every NiO_6 unit aligns uniformly along the y axis.

$LiNiPO_4$ single crystals were grown by the flux method [37]. Optical absorption measurements in the wavelength region of $380 < \lambda < 1690$ nm were carried out using a homebuilt fiber-based optical system [17]. The details of the experiments are given in the Supplemental Material [38]. The crystal structures in Fig. 2 were drawn by using VESTA software [39].

First, we present our main experimental results of a spontaneous SWIR OD effect (Fig. 3). Because OD signals are opposite in sign between a pair of antiferromagnetic domains (A+ and A−) in the LTC phase [compare Figs. 2(a) and 2(b)], one of the two domains must be selected to observe a finite OD signal. For $LiNiPO_4$, it is possible by cooling a sample with a magnetic field (H_{cool}) only through the transition at T_{N1} [36], likely owing to a tiny spontaneous magnetization along the c axis [40]. For this reason, we carried out the field cooling procedure with $H_{cool} = +5(+H_{cool})$ and $H_{cool} = -5$ kOe$(-H_{cool})$ along the c axis, removed the H_{cool} to observe a spontaneous effect, and then measured absorption coefficient (α) spectra in the SWIR region at 5 K. Figure 3(a) shows the results for

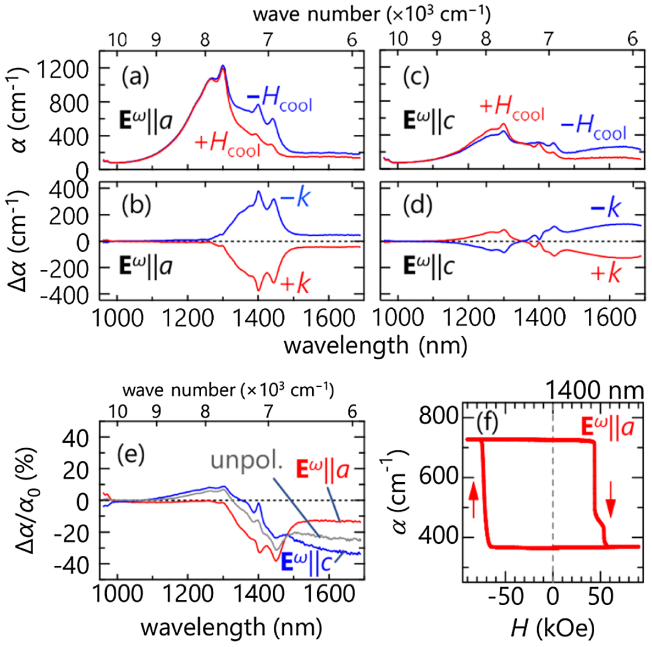

FIG. 3. The optical diode effect and its nonvolatile switching. (a) Absorption coefficient (α) spectra for $\mathbf{E}^{\omega}\|a$ and $\mathbf{k}\|+b$. The red and the blue-colored data were obtained after the field cooling procedure with $H_{\rm cool} = +5(+H_{\rm cool})$ and -5 kOe$(-H_{\rm cool})$, respectively. The $H_{\rm cool}$ was removed before each measurement to examine a nonvolatile effect. (b) Subtraction absorption spectra $\Delta\alpha = \alpha(+H_{\rm cool}) - \alpha(-H_{\rm cool})$ for $+k$ ($\mathbf{k}\|+b$, red curve) and $-k$ ($\mathbf{k}\|-b$, blue curve). (c),(d) Spectra of α (c) and $\Delta\alpha$ (d) at for $E^{\omega}\|c$ measured in the same manner as in (a) and (b), respectively. (e) $\Delta\alpha/\alpha_0$ spectra at for $\mathbf{E}^{\omega}\|a$ (red), $\mathbf{E}^{\omega}\|c$ (blue) and unpolarized light (gray curve). (f) Isothermal magnetic-field (H) dependence of α for $\mathbf{E}^{\omega}\|a$ at 1400 nm in $\mathbf{H}\|c$, measured after the cooling procedure with $+H_{\rm cool}$. All the data presented here were measured at 5 K.

light ($\mathbf{k}\|b$) linearly polarized along the a axis ($\mathbf{E}^{\omega}\|a$). Significantly, α spectra for the sample cooled with $+H_{\rm cool}$ and $-H_{\rm cool}$ [red and blue curves in Fig. 3(a)] exhibit a large difference at the wavelengths above 1300 nm, which is more evident in a subtraction spectrum [$\Delta\alpha = \alpha(+H_{\rm cool}) - \alpha(-H_{\rm cool})$] [Fig. 3(b)]. The finite $\Delta\alpha$ is well explained in terms of the opposite signs of the OD effect between the A+ and A− domains. Furthermore, we observe a full reversal of the $\Delta\alpha$ spectrum upon switching between $\mathbf{k}\|+b \leftrightarrow \mathbf{k}\|-b$ [Fig. 3(b)], directly confirming that the finite $\Delta\alpha$ entirely comes from the OD effect. We also obtain similar results for an orthogonal polarization $\mathbf{E}^{\omega}\|c$, evidencing the OD effect for this polarization [see Figs. 3(c) and 3(d)].

Next, to quantify the magnitude of the observed OD effect, we calculate an absolute relative difference of α in a percentage, namely, $|\Delta\alpha/\alpha_0|$ [%], where $\alpha_0 = \alpha(+H_{\rm cool}) + \alpha(-H_{\rm cool})$. With this definition, an ultimate OD effect, that is, the one-way transparency, corresponds to $|\Delta\alpha/\alpha_0| = 100\%$. Figure 3(e) shows spectra of $\Delta\alpha/\alpha_0$. One can see that $|\Delta\alpha/\alpha_0|$ reaches ~40% at 1450 nm for $\mathbf{E}^{\omega}\|a$ and ~30% at 1670 nm for $\mathbf{E}^{\omega}\|c$, which exceed those of any reported spontaneous OD effects in the SWIR region, as seen in Fig. 1. Even for unpolarized light, $|\Delta\alpha/\alpha_0|$ reaches 30% at 1450 nm and retains high values (>20%) over a wide wavelength range from 1410 to at least 1690 nm. Therefore, the giant spontaneous SWIR OD effect is demonstrated for $LiNiPO_4$. We also emphasize a very large absolute magnitude of $\Delta\alpha \sim 400$ cm^{-1} at 1400 nm for $\mathbf{E}^{\omega}\|a$. To our knowledge, this is the largest among reported OD effects in any wavelength regions.

Furthermore, we show that this giant OD effect can be isothermally switched by a magnetic field. Figure 3(f) shows the magnetic field ($H\|c$) dependence of α at 1400 nm and 5 K measured after the cooling procedure with $+H_{\rm cool}$. It is seen that α exhibits a sharp hysteretic switching with a very large change of ~200% (from 370 to 720 cm^{-1}). This switching is ascribed to a flip of the tiny ferromagnetic component that leads to a switching between A+ and A− domains (i.e., a sign reversal of the OD effect), as indicated by magnetization measurements (see the Supplemental Material [38]). Moreover, the magnitude of α completely retains even at $H = 0$ and is robust to magnetic field cycling, demonstrating a nonvolatile switchable nature of the giant OD effect. Detailed temperature and magnetic-field dependent data of the OD effect can be found in the Supplemental Material [38].

Now we discuss the microscopic origin of the observed OD effect. As seen in Fig. 2(a), the unit cell of the $LiNiPO_4$ structure contains four crystallographically equivalent Ni^{2+} ions [labeled as Ni(l) with $l = 1$–4] surrounded by distorted oxygen octahedra forming NiO_6 units. First, we shall consider a contribution to the OD effect from each NiO_6 unit, $\Delta\alpha^l$, which is expressed as [11]

$$\begin{aligned}\Delta\alpha^l = \alpha^l_{+k} - \alpha^l_{-k} &\propto |\langle e|H_{\rm E1}|g\rangle + \langle e|H_{\rm M1}|g\rangle|^2 \\ &\quad - |\langle e|H_{\rm E1}|g\rangle - \langle e|H_{\rm M1}|g\rangle|^2 \\ &= 2\langle g|H_{\rm E1}|e\rangle\langle e|H_{\rm M1}|g\rangle + \text{c.c.} \qquad (1)\end{aligned}$$

Here, $H_{\rm E1}$ ($H_{\rm M1}$) is the E1 transition operator related to an electric (magnetic) component of light, $\mathbf{E}^{\omega}$ ($\mathbf{H}^{\omega}$). g (e) denotes the wave function of the ground (excited) state of each Ni(l). The true local site symmetry at each Ni(l) is C_v (m_y), but close to higher symmetry C_{2v} ($2_z m_x m_y$) [29]. Here, x, y, and z denote the local orthogonal coordinate, y is parallel to b, and z makes an angle of $\theta_{cz} \approx 35°$ with c [see Fig. 2(c)]. As a result, a local electric dipole $\mathbf{p}$ along the z axis can be defined on each NiO_6 unit [Fig. 2(d)]. It is known that noncollinear configuration of macroscopic $\mathbf{P}$ and $\mathbf{M}$ can lead to the OD effect for $\mathbf{k}\|(\mathbf{P}\times\mathbf{M})$ [2,3]. Similarly, the combination of mutually noncollinear $\mathbf{p}$ and $\mathbf{S}$ of each NiO_6 unit can lead to a local OD effect for $\mathbf{k}\|(\mathbf{p}\times\mathbf{S})\|y$. Note that the quantity $\mathbf{p}\times\mathbf{S}$ is identical for every NiO_6 unit [Fig. 2(d)], indicating that the OD effect of the whole system (i.e., $\Delta\alpha$) should be the sum of $\Delta\alpha^l$ over

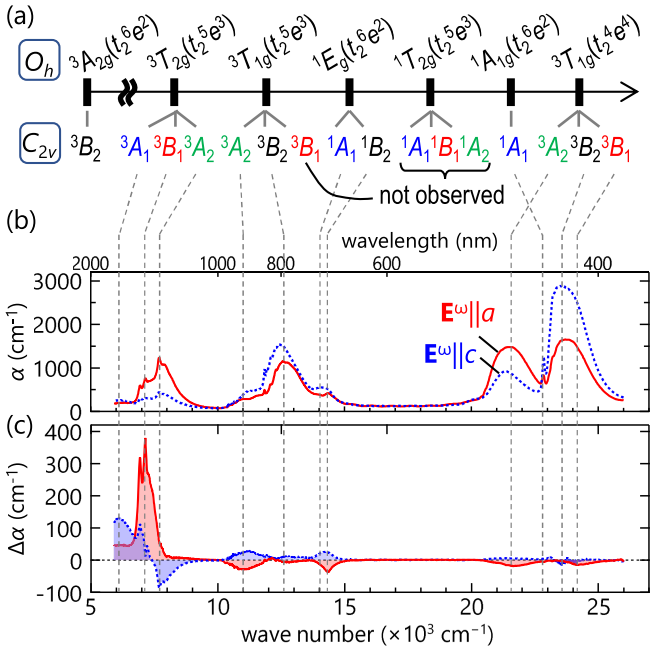

FIG. 4. (a) Energy scheme of Ni^{2+} orbital states for O_h and C_{2v} partly reproduced from [29]. (b),(c) Spectra of α (b) and $\Delta\alpha$ (c) for $\mathbf{E}^\omega \| a$ (red solid curve) and $\mathbf{E}^\omega \| c$ (blue dotted curve) measured at 5 K in the visible and near-infrared regions. The vertical dashed lines on absorption bands indicate the positions of respective Ni^{2+} orbital states shown in the panel (a).

$l = 1$–4. Therefore, considering an optical transition process on a single NiO_6 unit is sufficient to discuss the microscopic origin of the OD effect.

For a detailed consideration, we newly measure α and $\Delta\alpha$ spectra of a thinner sample in an extended region (400 ~ 1690 nm), the results of which are displayed in Figs. 4(b) and 4(c) as a function of wave number. The dashed lines on absorption bands indicate respective Ni^{2+} orbital states for O_h and C_{2v} according to an energy diagram proposed in Ref. [29] [see Fig. 4(a)]. Within the C_{2v} approximation, the ground state is $^3B_2$ [derived from $^3A_{2g}(t_2^6e^2)$ in O_h] hereafter denoted as $^3B_2^0$. Table I summarizes a selection rule for our experimental geometry with $\mathbf{k} \| y$, indicating that d-d transitions from $^3B_2^0$ to any excited states are either only E1 or only M1 allowed. However, the selection rule is relaxed by introducing the spin-orbit interaction (SOI) as it hybridizes the excited states. Of the components of $\mathbf{S}$, only the x component S_x [$=|\mathbf{S}| \sin(\theta_s + \theta_{cz})$] orthogonal to $\mathbf{p}$ is vital for the OD effect. Hence, we consider an L_xS_x term in the SOI, where L_x denotes an orbital angular momentum along the x axis. The L_xS_x term belongs to B_2 symmetry, which hybridizes the states A_1 and B_2. It also hybridizes the states A_2 and B_1. Consequently, the transitions to A_1 and those to B_2 become both E1 and M1 allowed for $\mathbf{E}^\omega \| z$ and $\mathbf{H}^\omega \| x$, while the transitions to A_2 and those to B_1 become both E1 and M1 allowed for $\mathbf{E}^\omega \| x$ and $\mathbf{H}^\omega \| z$. Therefore, all the transitions satisfy the criteria for the

TABLE I. Selection rule for transitions from the ground state $^3B_2^0$ to excited states (A_1, A_2, B_1, and B_2) in C_{2v}.

	A_1	A_2	B_1	B_2
E1 transition	$\mathbf{E}^\omega \| y$[a]	$\mathbf{E}^\omega \| x$	forbidden[b]	$\mathbf{E}^\omega \| z$
M1 transition	$\mathbf{H}^\omega \| x$	$\mathbf{H}^\omega \| y$	$\mathbf{H}^\omega \| z$	forbidden

[a]This means that the $^3B_2^0 \rightarrow A_1$ transition is E1 allowed with $\mathbf{E}^\omega \| y$.

[b]This means that the $^3B_2^0 \rightarrow B_1$ transition is E1 forbidden.

OD effect to emerge [2,6,7,11,14–17]. The OD effect should be observed both for the $\mathbf{E}^\omega \| a$ and $\mathbf{E}^\omega \| c$ polarized light since they possess both x and z components of $\mathbf{E}^\omega$ and $\mathbf{H}^\omega$ [Fig. 2(c)]. Indeed, the finite $\Delta\alpha$ signals are observed at most of absorption bands [Figs. 4(b) and 4(c)]. Thus, the observed OD effect can be explained in terms of Ni^{2+} d-d transitions within the C_{2v} approximation by considering the effects of SOI.

As described above, our strategy to achieve a large SWIR OD effect is based on the possibility of a significant M1 contribution to the $^3A_{2g}(t_2^6e^2) \rightarrow {}^3T_{2g}(t_2^5e^3)$ transition of Ni^{2+} in O_h symmetry [18,28–31]. As seen in Fig. 4(a), $^3T_{2g}(t_2^5e^3)$ of $LiNiPO_4$ is split into $^3A_1$, $^3B_1$, and $^3A_2$ by the $O_h \rightarrow C_{2v}$ distortion. Nonetheless, the results have shown that the transitions to $^3B_1$ and $^3A_1$ derived from $^3T_{2g}(t_2^5e^3)$ lead to the giant OD effect above ~1400 nm (below ~7000 cm^{-1}) (see Fig. 4). Therefore, a large SWIR OD effect can be anticipated in various Ni-based ME AFMs regardless of distortions of NiO_6 octahedral units.

Finally, we point out two factors which would further amplify the OD signals. The first one is on the spin structure. As discussed above, it is only the x component of $\mathbf{S}$ (orthognal to $\mathbf{p}$) that contributes to the OD effect. However, as seen in Fig. 2(c), the magnitude of S_x is largely reduced compared to that of $\mathbf{S}$ by a factor of $\sin(\theta_s + \theta_{cz}) \approx 0.7$. This suggests that making $\mathbf{S}$ orthogonal to $\mathbf{p}$ may amplify the OD signals. The second factor is on the crystal structure. As seen in Fig. 2(c), the global a and c axes and the local x and z axes are not parallel to each other due to a nonuniform orientation of the NiO_6 units or, in other words, a noncollinear arrangement of $\mathbf{p}$ [Fig. 2(d)]. As a result, the x- (z-) axis component of $\mathbf{E}^\omega$ ($\mathbf{H}^\omega$) is reduced compared to the magnitude of incident $\mathbf{E}^\omega \| a$ ($\mathbf{H}^\omega \| c$) by a factor of $\cos\theta_{cz} \approx 0.82$, which in turn reduces the magnitude of the observed $\Delta\alpha$ by a factor of $\cos^2\theta_{cz} \approx 0.67$ compared to the sum of $\Delta\alpha^l$. It is therefore implied that a collinear arrangement of $\mathbf{p}$ is favorable to enhance the OD effect. Combining the two factors, we propose that even larger OD effects can be achieved for a Ni-based ME AFM where Ni^{2+} spins and local electric dipoles of every NiO_6 unit are orthogonal and, respectively, form a collinear arrangement.

In conclusion, using the material exploration strategy based on the Ni^{2+} d-d transitions, we have achieved the

giant spontaneous optical diode effect at the shortwave infrared wavelengths in the magnetoelectric antiferromagnet $LiNiPO_4$. Moreover, we have demonstrated a nonvolatile switching of the optical diode effect with an applied magnetic field. Symmetry considerations suggest that the optical diode effect can be further enlarged by exploring a Ni-based magnetoelectric antiferromagnet where Ni^{2+} spins and local electric dipoles of every NiO_6 unit are orthogonal and respectively form a collinear arrangement. Thus, the present work may open a pathway to achieve nonvolatile switchable one-way transparency, which will find applications to novel nonreciprocal optical devices that can control the light propagation.

We thank Professor Dr. T. Arima for helpful discussion. K. K. acknowledges support from JSPS KAKENHI Grant No. JP19H01847, the MEXT Leading Initiative for Excellent Young Researchers (LEADER), the Murata Science Foundation, and the Iketani Science and Technology Foundation. T. K. acknowledges support from JSPS KAKENHI Grants No. JP19H05823, No. JP21H04436, and No. JP21H04988. This work was partly performed at the High Field Laboratory for Superconducting Materials, Institute for Materials Research, Tohoku University (Project No. 202112-HMKGE-0013).

*kentakimura@omu.ac.jp

[1] L. D. Barron and J. Vrbancich, Mol. Phys. **51**, 715 (1984).
[2] T. Arima, J. Phys. Condens. Matter **20**, 434211 (2008).
[3] D. Szaller, S. Bordács, and I. Kézsmárki, Phys. Rev. B **87**, 014421 (2013).
[4] G. L. J. A. Rikken and E. Raupach, Nature (London) **390**, 493 (1997).
[5] G. L. J. A. Rikken, C. Strohm, and P. Wyder, Phys. Rev. Lett. **89**, 133005 (2002).
[6] J. H. Jung, M. Matsubara, T. Arima, J. P. He, Y. Kaneko, and Y. Tokura, Phys. Rev. Lett. **93**, 037403 (2004).
[7] M. Saito, K. Taniguchi, and T. Arima, J. Phys. Soc. Jpn. **77**, 013705 (2008).
[8] Y. Shimada, H. Kiyama, and Y. Tokura, J. Phys. Soc. Jpn. **77**, 033706 (2008).
[9] I. Kézsmárki, D. Szaller, S. Bordács, V. Kocsis, Y. Tokunaga, Y. Taguchi, H. Murakawa, Y. Tokura, H. Engelkamp, T. Rõõm, and U. Nagel, Nat. Commun. **5**, 3203 (2014).
[10] I. Kézsmárki, U. Nagel, S. Bordács, R. S. Fishman, J. H. Lee, H. T. Yi, S.-W. Cheong, and T. Rõõm, Phys. Rev. Lett. **115**, 127203 (2015).
[11] S. Toyoda, N. Abe, S. Kimura, Y. H. Matsuda, T. Nomura, A. Ikeda, S. Takeyama, and T. Arima, Phys. Rev. Lett. **115**, 267207 (2015).
[12] S. Yu, B. Gao, J. W. Kim, S.-W. Cheong, M. K. L. Man, J. Madéo, K. M. Dani, and D. Talbayev, Phys. Rev. Lett. **120**, 037601 (2018).
[13] V. Kocsis, K. Penc, T. Rõõm, U. Nagel, J. Vít, J. Romhányi, Y. Tokunaga, Y. Taguchi, Y. Tokura, I. Kézsmárki, and S. Bordács, Phys. Rev. Lett. **121**, 057601 (2018).
[14] M. O. Yokosuk, H.-S. Kim, K. D. Hughey, J. Kim, A. V. Stier, K. R. O'Neal, J. Yang, S. A. Crooker, K. Haule, S.-W. Cheong, D. Vanderbilt, and J. L. Musfeldt, npj Quantum Mater. **5**, 20 (2020).
[15] T. Sato, N. Abe, S. Kimura, Y. Tokunaga, and T. H. Arima, Phys. Rev. Lett. **124**, 217402 (2020).
[16] K. Kimura, T. Katsuyoshi, Y. Sawada, S. Kimura, and T. Kimura, Commun. Mater. **1**, 39 (2020).
[17] K. Kimura, Y. Otake, and T. Kimura, Nat. Commun. **13**, 697 (2022).
[18] K. Park, M. O. Yokosuk, M. Goryca, J. J. Yang, S. A. Crooker, S.-W. Cheong, K. Haule, D. Vanderbilt, H.-S. Kim, and J. L. Musfeldt, npj Quantum Mater. **7**, 38 (2022).
[19] X. Wu, M. Kim, H. Qu, and Y. Wang, Nat. Commun. **10**, 2672 (2019).
[20] K. B. Whetsel, Appl. Spectrosc. Rev. **2**, 1 (1968).
[21] Y. Yanase, J. Phys. Soc. Jpn. **83**, 014703 (2014).
[22] N. D. Khanh, N. Abe, H. Sagayama, A. Nakao, T. Hanashima, R. Kiyanagi, Y. Tokunaga, and T. Arima, Phys. Rev. B **93**, 075117 (2016).
[23] S. Hayami, H. Kusunose, and Y. Motome, J. Phys. Condens. Matter **28**, 395601 (2016).
[24] M. Shinozaki, G. Motoyama, M. Tsubouchi, M. Sezaki, J. Gouchi, S. Nishigori, T. Mutou, A. Yamaguchi, K. Fujiwara, K. Miyoshi, and Y. Uwatoko, J. Phys. Soc. Jpn. **89**, 033703 (2020).
[25] V. Baltz, A. Manchon, M. Tsoi, T. Moriyama, T. Ono, and Y. Tserkovnyak, Rev. Mod. Phys. **90**, 015005 (2018).
[26] P. Němec, M. Fiebig, T. Kampfrath, and A. V. Kimel, Nat. Phys. **14**, 229 (2018).
[27] G. R. Rossman, R. D. Shannon, and R. K. Waring, J. Solid State Chem. **39**, 277 (1981).
[28] R. Grinter, M. J. Harding, and S. F. Mason, J. Chem. Soc. A **0**, 667 (1970).
[29] A. Belletti, R. Borromei, R. Cammi, and E. Cavalli, Phys. Status Solidi B **163**, 281 (1991).
[30] R. Borromei, E. Cavalli, and L. Oleari, Inorg. Chim. Acta **204**, 159 (1993).
[31] M. Fiebig, D. Fröhlich, Th. Lottermoser, V. V. Pavlov, R. V. Pisarev, and H.-J. Weber, Phys. Rev. Lett. **87**, 137202 (2001).
[32] D. Vaknin, J. L. Zarestky, J.-P. Rivera, and H. Schmid, Phys. Rev. Lett. **92**, 207201 (2004).
[33] J. Li, T. B. S. Jensen, N. H. Andersen, J. L. Zarestky, R. W. McCallum, J.-H. Chung, J. W. Lynn, and D. Vaknin, Phys. Rev. B **79**, 174435 (2009).
[34] Thomas Bagger Stibius Jensen, N. B. Christensen, M. Kenzelmann, H. M. Rønnow, C. Niedermayer, N. H. Andersen, K. Lefmann, J. Schefer, M. V. Zimmermann, J. Li, J. L. Zarestky, and D. Vaknin, Phys. Rev. B **79**, 092412 (2009).
[35] R. Toft-Petersen, J. Jensen, Thomas Bagger Stibius Jensen, N. H. Andersen, N. B. Christensen, C. Niedermayer, M. Kenzelmann, M. Skoulatos, M. D. Le, K. Lefmann, S. R. Hansen, J. Li, J. L. Zarestky, and D. Vaknin, Phys. Rev. B **84**, 054408 (2011).

[36] I. Kornev, M. Bichurin, J.-P. Rivera, S. Gentil, H. Schmid, A. G. M. Jansen, and P. Wyder, Phys. Rev. B **62**, 12247 (2000).
[37] V. I. Fomin, V. P. Gnezdilov, V. S. Kurnosov, A. V. Peschanskii, A. V. Yeremenko, H. Schmid, J.-P. Rivera, and S. Gentil, Low Temp. Phys. **28**, 203 (2002).
[38] See Supplemental Material at http://link.aps.org/supplemental/10.1103/PhysRevLett.132.036901 for experimental details and additional experimental data.
[39] K. Momma and F. Izumi, J. Appl. Crystallogr. **44**, 1272 (2011).
[40] Yu. N. Kharchenko, N. F. Kharcheno, M. Baran, and R. Szymczak, Low Temp. Phys. **29**, 579 (2003).